IV. CONCLUSION

The design of a single-feed square-ring patch antenna with switchable radiation patterns has been presented and studied. The antenna structure has four shorting walls in which two shorting walls are directly connected to the radiating patch, and the connection states of the other two shorting walls can be switched electrically by pin diodes. When the diodes are ON, the antenna is operated at the monopolar plate-patch mode that can radiate conical patterns; on the other hand, the antenna is operated at the TM_{11} mode that can radiate broadside patterns when the diodes are OFF. Moreover, the two modes can be designed at the same resonant frequency by adjusting the width of the shorting walls. An antenna prototype operated at 2020 MHz has been successfully implemented. From the experimental results, it is found that the main-beam positions of the radiation patterns are directed at the elevation angles of $50°$ and $0°$ when the diodes are ON and OFF, respectively. This characteristic not only allows the antenna to have the attractive feature of pattern diversity but also makes the antenna easy to provide hemispherical coverage for indoor mobile communication systems. Moreover, the proposed antenna is easily integrated with RF circuits.

REFERENCES

[1] W. H. Chen and Z. H. Feng, "Planar reconfigurable pattern antenna by reactive-load switching," *Microw. Opt. Technol. Lett.*, vol. 47, pp. 506–507, Dec. 5, 2005.

[2] L. Low and R. J. Langley, "Single feed antenna with radiation pattern diversity," *Electron. Lett.*, vol. 40, pp. 975–976, Aug. 5, 2004.

[3] S. Nikolaou, R. Bairavasubramanian, C. Lugo, I. Carrasquillo, D. C. Thompson, G. E. Ponchak, J. Papapolymerou, and M. M. Tentzeris, "Pattern and frequency reconfigurable annular slot antenna using pin diodes," *IEEE Trans Antennas Propag.*, vol. AP-54, pp. 439–448, Feb. 2007.

[4] G. H. Huff, J. Feng, S. Zhang, and J. T. Bernhard, "A novel radiation pattern and frequency reconfigurable single turn square spiral microstrip antenna," *IEEE Microw. Wireless Comp. Lett.*, vol. 13, pp. 57–59, 2003.

[5] S. L. S. Yang and K. M. Luk, "Design of a wide-band L-probe patch antenna for pattern reconfiguration or diversity applications," *IEEE Trans. Antennas Propag.*, vol. AP-54, pp. 433–438, Feb. 2006.

[6] J. S. Row, S. H. Yeh, and K. L. Wong, "A wideband monopolar plate-patch antenna," *IEEE Trans. Antennas Propag.*, vol. AP-50, pp. 1328–1330, Sept. 2002.

[7] C. W. Su, J. S. Row, and J. F. Wu, "Design of a single-feed dual-frequency microstrip antenna," *Microw. Opt. Technol. Lett.*, vol. 47, pp. 114–116, Oct. 20, 2005.

[8] C. Y. D. Sim, J. S. Row, and M. Y. Chen, "Characteristics of superstrate-loaded circular polarization square-ring microstrip antennas on thick substrate," *Microw. Opt. Technol. Lett.*, vol. 47, pp. 567–570, Dec. 20, 2005.

[9] J. S. Row and S. W. Wu, "Monopolar square patch antennas with wideband operation," *Electron. Lett.*, vol. 42, pp. 17–18, Feb. 2, 2006.

[10] C. Delaveaud, P. Leveque, and B. Jecko, "New kind of microstrip antenna: The monopolar wire-patch antenna," *Electron. Lett.*, vol. 30, pp. 1–2, Jan. 6, 1994.

[11] S. H. Yeh and K. L. Wong, "A broadband low-profile cylindrical monopole antenna top loaded with a shorted cross patch," *Microw. Opt. Technol. Lett.*, vol. 32, pp. 186–188, Feb. 5, 2002.

A Modified Model-Based Interpolation Method to Accelerate the Characterization of UWB Antenna System

Z. Zhang and Y. H. Lee

Abstract—The persisting problem associated with ultrawideband (UWB) antenna design is the lack of an efficient method to characterize the antenna system. In this paper, the characteristics of the antenna system are described by a transfer function. In order to alleviate the computation intensity, a modified model based parameter estimation method is applied to the rational modeling of the transfer function by employing the intrinsic features of the UWB antenna system. With this modified rational modeling method, only a small quantity of samples is needed to give a complete representation of the performance of the UWB antenna system. Therefore, the characterization of the UWB system is largely accelerated while maintaining results with high accuracy.

Index Terms—Model based parameter estimation, transfer function, ultrawideband (UWB) antenna system.

I. INTRODUCTION

In UWB communications, the antenna system plays a dominating role of filtering. Thus, instead of the traditional approaches, it should be examined from a filtering point of view. The transfer function (TF) method proposed in [1], [2], [12] has the capability of doing so. The TF is defined as the ratio of the received voltage to the transmitted voltage as in [1]

$$H(\omega) = \frac{V_r(\omega)}{V_t(\omega)}. \tag{1}$$

In the existing literature, the transfer function is obtained from either experimental measurements [3], [4] or numerical simulations [5], [6]. The analysis of UWB antenna system is principally based on time domain and frequency domain calculations. Finite-difference time-domain (FDTD) [7] and method of moments (MoM) [8] are two of the most frequently used methods in each category. In practice, FDTD is more efficient as it can perform a broadband analysis in a single simulation. However, FDTD has to be modified every time the pulse shape is changed. If pulse shaping is taken into account as part of the system optimization, the efficiency of MoM becomes comparable to that of FDTD. In addition, MoM has the advantage of its flexibility in geometrical modeling. Therefore, in this paper, MoM is chosen as the computation method used to calculate the TF. The calculation of the TF over the UWB band using MoM is time-consuming. To alleviate such computational difficulties, an interpolation model known as the model-based parameter estimation (MBPE) is used [9]. In practice, the modeling complexity is increased with the extension of the bandwidth. Thus, it is difficult or even impossible to realize the modeling of an antenna system with ultrawide bandwidth. However, by taking advantage of the features that the TF exhibits, a modified model based method can be used to evaluate the TF such that it will give a good representation of these features and therefore can aid in speeding up the modeling process. As a result, the system characterization is expedited several-fold.
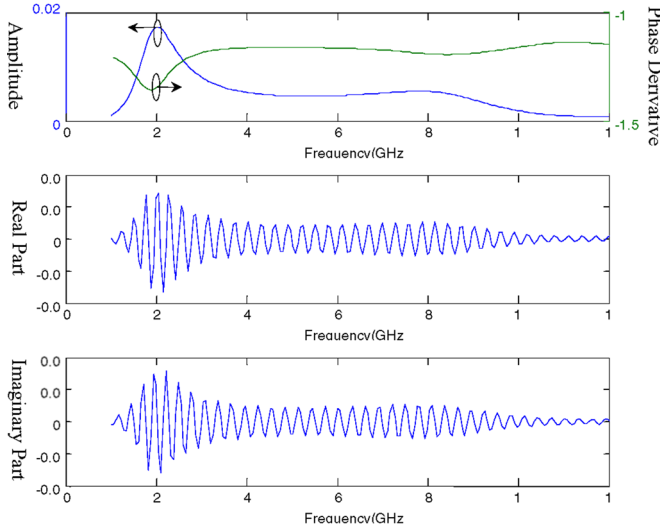
Fig. 1.   Comparisons of complexity of the transfer function.

II. MODIFIED MBPE METHOD

MBPE is a numerical process which uses a physical based model to construct a highly efficient representation/approximation of EM properties of interest. In this paper, a rational polynomial given by (2) is used as the fitting model to the TF [9]

$$H(\omega) = \frac{N_m(s)}{D_n(s)} = \frac{N_0 + N_1 s + \cdots + N_m s^m}{D_0 + D_1 s + \cdots + D_n s^n} \qquad (2)$$

where $H(\omega)$ is evaluated along the complex frequency domain where $s = j\omega = j2\pi f$. The coefficients in the numerator and denominator polynomials are N_i for $i = 0 : m$ and D_j for $j = 0 : n$ with orders m and n, respectively. By setting $D_n = 1$ and $m = n$ as a default, $H(\omega)$ has $2m + 1$ unknown complex coefficients which are estimated through a curve fitting technique [10] using simulation data obtained from the MOM solver [11]. As expected, the sampling technique and the number of sample points are crucial to the accurate modeling of the TF. In this paper, uniform sampling is adopted for its simplicity. The number of samples needed is directly proportional to the bandwidth. Thus, the accurate modeling of a UWB antenna system requires large number of samples which implies large computation time and complexity.

For an ideal UWB antenna system, the amplitude and the ground delay of its TF is expected to be invariant over the entire operating band as shown in Fig. 1. Therefore, any antenna used for UWB communication is often electrically small such that the variations of the amplitude and the phase derivative are expected to be small despite the complexity within the real and imaginary part of the TF. An example is given in Fig. 1 to illustrate this point.

The TF between two bowtie antennas is shown in Fig. 1. It can be seen that its amplitude and phase derivative exhibit smooth variations, whereas its real and imaginary part suffer significant wavelike changes across the frequency band of 1–12 GHz. It indicates that the quantity of samples required to guarantee a reliable description of amplitude and phase derivatives is much smaller than that required for the fitting of real/imaginary part of the TF. This inspired the idea of approaching the overall modeling of the TF from the development of a model that can give an accurate representation of both the amplitude and the phase derivative. This model, based on the MBPE method, only relies on a few sample points thus eliminating the difficulty encountered by traditional modeling where large numbers of sample points are needed. By comparison, the variation of the amplitude is generally smaller than

that of the phase derivative, so the number of samples required for amplitude representation is a good estimation for the possible minimum number of samples required for the modified MBPE method to represent the TF. Therefore, it is wise to find a model with accurate amplitude information initially. Assuming that the rational function R_a in (3), which was established using a limited number of samples, can give an accurate representation of the amplitude, A. However, in (3), there still exist uncertainties within the phase information

$$R_a(\omega) = \frac{\sum_{k=0}^{m} N_k s^k}{\sum_{k=0}^{n} D_k s^k} = A e^{j(p_0 + \int_{\omega_0}^{\omega} p'_a \, d\omega)} \qquad (3)$$

$$R_e(\omega) = A e^{j(p_0 + \int_{\omega_0}^{\omega} p'_e \, d\omega)} \qquad (4)$$

where p_0 refers to the phase at the starting angular frequency ω_0, p'_a, and p'_e denote the phase derivatives of R_a and R_e with respect to ω, respectively.

In order to give a complete representation of the TF with the accurate amplitude and phase, (4) can be used. While R_a and R_e are identical in terms of their amplitude, the difference between them resides in the p'_a and p'_e. Since R_a is capable of predicting the amplitude of R_e, there is an underlying connection between R_e and R_a. In other words, there exists an implicit relationship between p'_a and p'_e. It is verified that a linear relationship does exist between the continuous unwrapped (with a 2π phase) p'_a and p'_e given in (5), where a is a constant

$$p'_e(\omega) = p'_a(\omega) + a. \qquad (5)$$

It can be seen from (5) that p'_a fails to represent p'_e exactly since the complexity of the phase derivative is relatively higher with the exception of the special case when $a = 0$. However, the second derivative p''_e is always considerably smoother over the entire band. Thus, R_a is able to depict p''_e accurately from a physical point of view. By taking the derivatives of (5)

$$p''_e(\omega) = p''_a(\omega). \qquad (6)$$

As shown in (6), the p''_a is exactly equal to p''_e and can be used to derive R_e with a reasonable amount of accuracy.

Suppose R_a is already known, p'_a can be easily calculated at any point. Using (5), the constant a can be estimated using only two frequency points with an exact solutions of phase derivative p'_e, no matter which frequency point is picked. The derivation of p'_e at a point requires the additional computation of the TF at that point and the point adjacent to it in order to their extract the phases. If the point is chosen to be one of the samples used to model R_a, only one adjacent point needs to be calculated. Theoretically, at any sampled frequency ω_s where $R_a(\omega_s)$ is equal to $R_e(\omega_s)$, using (3), (4), and (5), a must then satisfy (7). If the estimate of a can result in an appropriate integer of n to satisfy (7), the reliability of the formulation can be justified and the exact value of a can be achieved corresponding to the specific n

$$e^{ja\Delta\omega_s} = 1 \Rightarrow a = \frac{2n\pi}{\Delta\omega_s}. \qquad (7)$$

The above analysis is based on the assumption that R_a is well modeled using a limited amount of samples. When it comes to the rational modeling of R_a, several questions arise.

1) The Number of Sample Points N_s, and the Order of the Rational Function m: The number of samples N_s, depends on both the bandwidth and the variation of amplitude with frequency. From empirical studies, the proper number of samples for most UWB antenna is about 3 to 4 samples per 1 GHz. Therefore, given a specified bandwidth, the number of samples required can be approximated. Having chosen the number of samples, the maximum allowable order is therefore confined to $(m \leqslant (N_s - 1)/2)$ [9]. In general, the appropriate value of m is close to the maximum allowable order and can be found in the vicinity

of this limit. An example of the properties of N_s and m is given in Section III.

2) Criteria for Evaluating the Performance of the Fitting Model: These criteria are defined to estimate the performance of the model and to guide the improvement in the values of N_s and m.

a) The $\mathrm{GE_{max}}$ *Criterion Is Taken as the First Criterion:*

$$\Delta\mathrm{GE}_i(f_s) = \frac{|G(f_s) - M_i(f_s)|}{|G(f_s)| + |M_i(f_s)|}. \qquad (8)$$

$G(f_s)$ and $M_i(f_s)$ represents the sampled and calculated data by the model i at the sampled frequency f_s. $\Delta\mathrm{GE}_i(f_s)$ is an indication of how accurate the rational TF is to the actual data. A threshold value is defined such that if $\Delta\mathrm{GE}_i(f_s)$ is greater than this threshold, the accuracy of the frequency points within a sample interval to the sampled frequency, f_s is classified as uncertain. In order to evaluate the fitness of the model over the entire frequency range of interest, the maximum error amongst $\Delta\mathrm{GE}_i(f_s)$ is referred to as the $\mathrm{GE_{max}}$ criterion

$$\mathrm{GE_{max}} = \max(\Delta\mathrm{GE}_i). \qquad (9)$$

b) The $\Delta\kappa_i$ *Criterion is Taken as the Second Criterion:* While the sampled data might not contain sufficient information to represent the overall behavior of the TF, the abrupt changes where the smoothness of the TF is impaired give a good indication of the regions with uncertainty. In view of this, the curvature of the TF is computed by

$$\Delta\kappa_i(f_c) = \frac{|Y_i(f_c)''|}{(1 + (Y_i(f_c)')^2)^{\frac{3}{2}}}$$
$$\text{where } Y_i(f_c) = \frac{|M_i(f_c)| - |M_{i\min}|}{|M_{i\max}| - |M_{i\min}|} \qquad (10)$$

where $Y_i(f_c)$ is the normalized magnitude at the calculated frequency f_c. The $\Delta\kappa_i$ criterion is also used to detect regions where the accuracy is questionable. Suppose, within a sample interval, there is a sample point where $\Delta\kappa_i$ exceeds a specified threshold, the accuracy of all the points within that sample interval is classified as uncertain.

A model that does not satisfy the $\mathrm{GE_{max}}$ criterion is definitely rejected as it is an essential requirement for a desired model. However, a model is still considered acceptable even if it has points that do not satisfy the $\Delta\kappa_i$ criterion since the "spikes" (causing it to fail the $\Delta\kappa_i$ criterion) might be a result of the physical nature of the antenna system. As a precaution, extra computation is required so as to check the cause of the "spike." The κ_{rms} criterion is an indicator for the smoothness of the overall model

$$\kappa_{\mathrm{rms}} = \sqrt{\sum \Delta\kappa_i^2}. \qquad (11)$$

Starting with the initial chosen number of samples, a group of models with reasonable order is calculated. The above two criteria are then checked and the models are classified into several categories according to their individual performances.

**If (NONE of the models satisfy the required $\mathrm{GE_{max}}$ criterion)**

The number of samples is updated and the samples are redistributed. To save computation cost, the new samples will be represented by the model with the lowest $\mathrm{GE_{max}}$ value from the former group, except for the samples with uncertainty. Those samples with uncertainty will be computed directly using the MoM. With the new samples, the process is repeated until a satisfactory model is found.
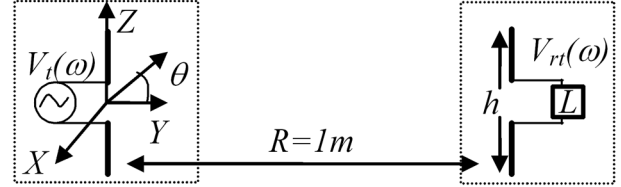**Otherwise**

   If (NONE of the models have points whose accuracy is uncertain)
   The model with the minimum κ_{rms} is determined as the desired model, and the process ends.
   Otherwise
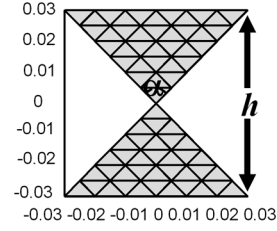
Fig. 2. (a) Meshed model of bowtie antenna (b) Setup of transmitter/receiver.

*The samples are updated by increasing the number of samples. Subsequently, the exact solutions of samples whose accuracy is classified as uncertain are compared with the calculated results from the model with the minimum κ_{rms} and the errors are calculated. **If (the errors are tolerable)***
The model is accepted. And the process comes to an end.
Otherwise
The process is continued until the criteria are met or the maximum number of iterations is reached.

In most cases, a desired fitting model can be obtained after a few slight modifications.

III. EXPERIMENTAL RESULTS AND ANALYSES

A generic communication system with two bowtie antennas is presented here as a numerical example. A simple bowtie model can be determined entirely by the height, h and the apex angle, α as shown in Fig. 2(a). The antenna system is investigated using MoM with MATLAB [11]. It comprises two identical bowtie antennas with $h = 0.06$ m and $\alpha = 90°$. They are directed towards each other in the same polarization at a distance of 1 m apart ($\theta = 90°$, $R = 1$ m). The TF at frequency ω is taken as the $V_r(\omega)$ while retaining $V_t(\omega)$ constant at 1 V. First, the model providing the precise amplitude representation of the TF is built. The acceptable model should satisfy the requirement of $\mathrm{GE_{max}} < 1\%$, and the threshold of the $\Delta\kappa_i$ criterion of 0.1.

As shown in Fig. 3, the frequency range of interest is increased from a bandwidth of 2 GHz to a bandwidth of 11 GHz with a bandwidth step increment of 3 GHz. The number of samples required to satisfy the $\mathrm{GE_{max}}$ criterion also increases. The ratio of the optimal number of samples to the bandwidth (N_s/B) is within the range of 3 to 4 samples per GHz and the suitable order is found to be close to the maximum allowable $((N_s - 1)/2)$. If fewer than 3 samples are used, the accuracy of the model is compromised, and if more than 4 samples are used, the computation complexity is increased unnecessarily. It can also be observed that with the increase in bandwidth, the value of $\mathrm{GE_{max}}$ for the optimal model also increases, which means the modeling complexity increases as well.

If the initially chosen number of samples fails to produce the desired result, modifications are done according to the criteria explained before. As illustrated in Fig. 4, a rational modeling is performed on an antenna system that operates from 1 to 4 GHz. Initially, the minimal empirical value of 9 ($N_s/B = 3$) is chosen as the number of samples required. Using these 9 samples, the formulated result (dot line) has a
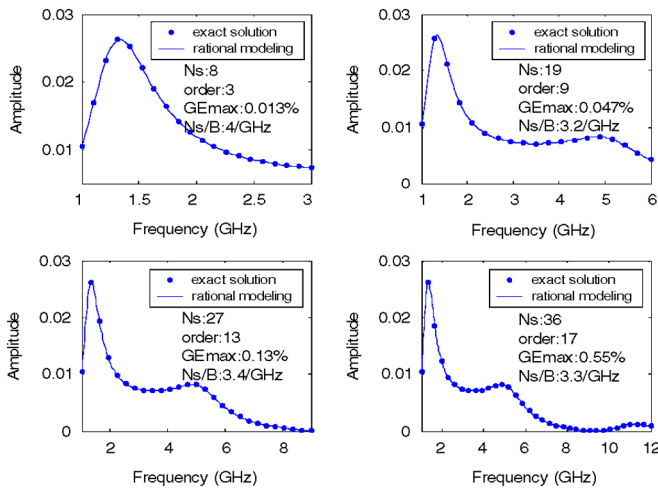
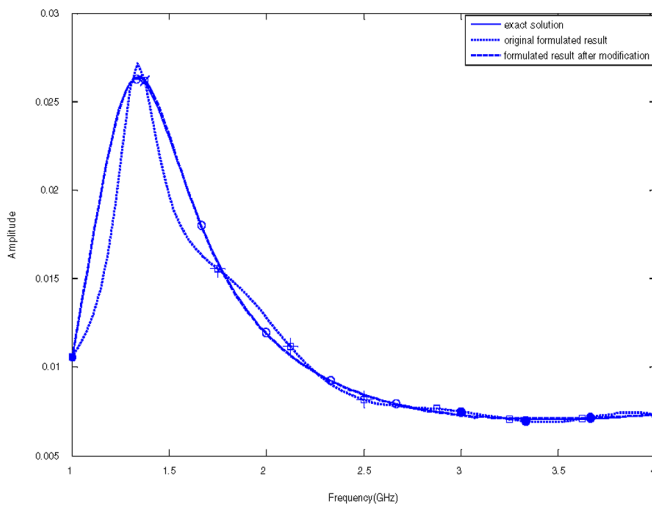Fig. 3. Relationship between the number of samples and the bandwidth.

Fig. 4. Modification scheme.

$GE_{\max} = 2.29\%$ which does not match the exact solution (solid line) well. Then, the number of samples is increased to 10. Judged by the $GE_{\max}$ and $\Delta\kappa_i$ criteria, the formulated solutions at the sampled frequencies "□" found to be uncertain are picked out and marked using "+" and "×" respectively. The solutions marked with "+" are the ones where $\Delta GE > 1\%$. And the other marked with "×" indicates a sample interval with points having $\Delta\kappa_i > 0.1$. All adjacent sample points within the sample interval of these sample frequency points are also classified as uncertain.

Therefore, the re-sampled data points "○" from these regions are calculated using MoM directly. The other data points marked "•" are calculated using the previously formulated rational model so as to save computation time. Using these 10 new samples, the result (dash line) with an order m, of 4 is satisfactory with $GE_{\max} = 0.3\%$.

For the UWB antenna system, the frequency range of interest extends from 1 to 12 GHz covering the FCC specified communication band (3.1–10.6 GHz). Interpolation over such a wide frequency band is achieved using the proposed method. Initially, 36 sample points are uniformly distributed over the frequency band of interest, 1–12 GHz. With an order of 17, a satisfactory model R_a is obtained as seen from Fig. 5. The $GE_{\max}$ value of this model is 0.55% which means that the maximum mismatch of the TF model with the actual result does not exceed 0.55%. In this model, a sharp peak emerges around 1 to 1.5 GHz.
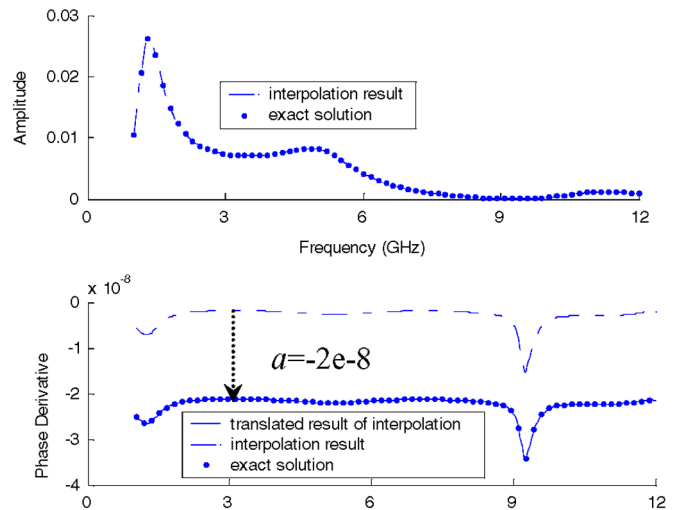

Fig. 5. Amplitudes and phase derivatives of the interpolated and extrapolated rational model.
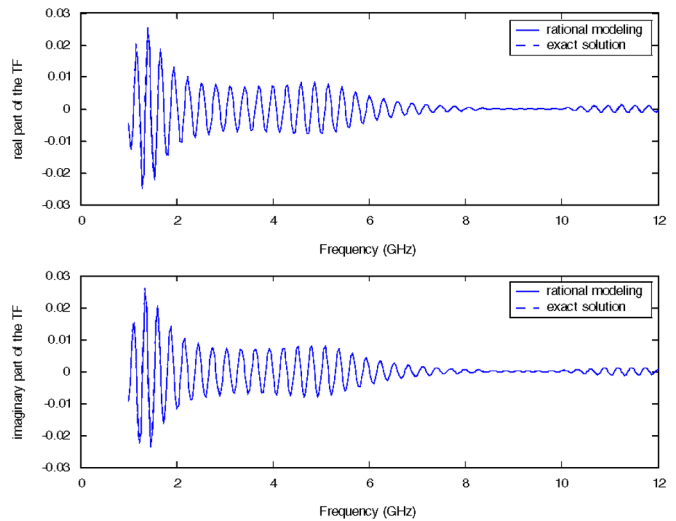

Fig. 6. Real and imaginary part of the transfer function.

This was detected in terms of the $\Delta\kappa_i$ criterion where a maximum $\Delta\kappa_i$ of 0.12, slightly surpassing the threshold of 0.1, was found. However, this "spike" was then validated to be a physical behavior of the antenna system through subsequent computation. This also demonstrates that the model has the capability of representing the physical behavior of the structure completely even around regions with abrupt changes. Also in Fig. 5, p'_a (dash-dot) of the interpolation model is plotted. As noted before, once p'_e of a point is known, the value of a can be addressed. According to the different reference points selected, the estimate of a might be slightly different from each other if the model is reliable enough. Therefore, they all correspond to a single value of n and finally result in the same exact solution of a. Considering the estimate of a can used to check the reliability of the formulation, as a rule of thumb, we choose to calculate p'_e at the point where the biggest curvature of $\Delta\kappa_i$ is generated. It is well-understood that the point is prone to be problematic and therefore, if the estimated value of a at that point can find a reasonable n to satisfy (7), it gives convincing evidence to the credibility of the entire model. In this case, a is estimated at the proposed point and the result is around $-2e - 8$. When multiplied by Δf_s $(=11e9/35)$, the value is close to -2π with $n = -1$. This justifies (7) and thereby strongly verifies that the modeling result

is reliable. Using (5), its translated solution (solid) approximates the exact solution well. The above examples fully demonstrate that the assumptions and modifications made in previous section are effective and efficient for the generation of an accurate interpolation model for UWB antenna systems.

Given the starting phase and phase derivative, the real and imaginary part of the TF can be determined. As seen from Fig. 6, the exact solution and formulated solution agree well. The property of the real or imaginary part is much more complicated than that of amplitude or phase derivative. While constructing a fitting model in the traditional sense so as to depict the real and imaginary parts of the TF, the number of samples has to be increased to 120. Therefore, using the modified method, the computation time is reduced by a factor of approximately $3.3\ (=120/36)$, but the accuracy is still maintained. This demonstrates the effectiveness and efficiency of the modified method in the modeling of the TF as compared to traditional methods.

IV. CONCLUSION

In this paper, an efficient and effective method for UWB antenna system characterization is introduced. Using this method, the comprehensive performance of the UWB antenna system can be represented by a simple rational formulated transfer function. A small number of samples are adequate to accurately represent the antenna system so that the computation time is greatly reduced. In conclusion, the proposed method not only resolves the difficulties in giving a comprehensive characterization of UWB antenna system but also speeds up the accurate simulation of the complete system.

REFERENCES

[1] Z. N. Chen, X. H. Wu, N. Yang, and M. Y. W. Chia, "Design considerations for antennas in UWB wireless communication systems," in *Proc. IEEE Int. Symp. Antennas and Propagation*, 2003, vol. 1, pp. 882–825.

[2] S. Zwierzchowski and M. Okoniewski, "Antennas for UWB communications: A novel filtering perspective," in *Proc. IEEE Int. Symp. Antennas and Propagation*, 2004, vol. 3, pp. 2504–2507.

[3] X. Qing and Z. N. Chen, "Transfer functions measurement for UWB antenna," in *Proc. IEEE Int. Symp. Antennas and Propagation*, 2004, vol. 3, pp. 2532–2535.

[4] Y. Shi, S. Aditya, and C. L. Law, "Transfer function characterization of UWB antennas based on frequency domain measurement," in *Eur. Microwave Conf.*, 2005, vol. 3, pp. 1735–1738.

[5] D. Manteuffel and J. Kunisch, "Efficient characterization of UWB antennas using the FDTD method," in *Proc. IEEE Int. Symp. Antennas and Propagation*, 2004, vol. 2, pp. 1752–1755.

[6] X. H. Wu and Z. N. Chen, "Design and optimization of UWB antennas by a powerful CAD tool: PULSE KIT," in *Proc. IEEE Int. Symp. Antennas and Propagation*, 2004, vol. 2, pp. 1756–1759.

[7] A. Taflove, *Computational Electrodynamics: The Finite-Difference Time-Domain Method*. Boston, MA: Artech House, 2000.

[8] E. K. Miller, *Computational Electromagnetics: Frequency-Domain Method of Moments*. New York: IEEE Press, 1992.

[9] E. K. Miller, "Model-based parameter estimation in electromagnetics—Part I: Background and theoretical development," *IEEE Antennas Propag. Mag.*, vol. 40, pp. 42–52, 1998.

[10] M. H. Richardson and D. L. Formenti, "Parameter estimation from frequency response measurements using rational fraction," in *Proc. 1st Int. Modal Analysis Conf.*, 1982, pp. 167–182.

[11] S. N. Makarov, *Antenna and EM Modeling with Matlab*. New York: Wiley-Interscience, 2002.

[12] H. Poor, *An Introduction to Signal Detection and Estimation*. New York: Springer-Verlag, 1985, ch. 4.

Off-Axis Performances of Half Maxwell Fish-Eye Lens Antennas at 77 GHz

Benjamin Fuchs, Olivier Lafond, Sébastien Rondineau, Mohamed Himdi, and Laurent Le Coq

Abstract—The off-axis performances at 77 GHz of multilayered half Maxwell fish-eye (HMFE) lenses fed by an open-ended waveguide is describes. When moving the feed with respect to (w.r.t.) the lens, it is shown that at least 40° of scanning can be achieved. Several off-axis configurations of the lens antenna are investigated and compared using a full-wave electromagnetic software. The directivity, far field pattern and scan angle of the lens antenna are reported for a rectilinear and angular off-axis displacement of the feed and also for various distances between the feed and the lens. It is also shown that a three-shell lens is good enough to achieve a wide scan angle. Finally, off-axis measurements done with a three-shell 6.15 λ_0-diameter HMFE lens antenna are compared to computed results to validate the simulations.

Index Terms—Automotive radars, lens antennas, millimeter-wave antenna, multiple-beam antennas.

I. INTRODUCTION

Many millimeter-wave communication and radar systems need compact antennas which possess a high gain and can form multiple beams. Examples are point-to-point and point-to-multipoint links [1], ground station for satellites [2], satellite multimedia communications, automotive radars [3], etc.

In this paper, a collision avoidance system with an operating frequency of 77 GHz will be the primary focus. For such systems, the antenna needs to be compact in order to be easily embedded. Moreover, the antenna has also to present a high gain to achieve a long range detection and for power budget reasons. Thus, focusing devices such as lens antennas are especially well suited because they exhibit low losses compared to printed technology in this frequency range. The ability to steer the beam is also required to better anticipate when the road turns for instance. This beam scanning can be achieved either electronically with phase shifters for continuous scanning or with switches for discrete scanning. In addition, one can mechanically move the feed with respect to (w.r.t.) the lens.

Various type of lens antennas have already been investigated for automotive radars. A spherical teflon lens fed by tapered slots antennas where the beam scanning can be achieved by switching between the antennas has been proposed by Schoenlinner [3]. Gallée [4] has suggested to use an artificial lens consisting of stacked parallel-plate waveguides of various lengths fed by a moving waveguide to steer the beam.

We choose to use an inhomogeneous hemispherical lens antenna, namely the half Maxwell fish-eye (HMFE) lens, fed by an open-ended waveguide. The beam scanning is performed mechanically for reliability, loss efficiency and cost reasons compared to the electronically scanning. The on-axis performances of the HMFE lens at 77 GHz have